Study of different features of fission dynamics of ^{224}Th produced in fusion reactions within a stochastic approach

H. Eslamizadeh[1)]

Department of Physics, Persian Gulf University 75169, Bushehr, Iran

Abstract: The evaporation residue cross section anisotropy of the fission fragment angular distribution, pre-scission neutron multiplicity and the pre-saddle and post-saddle contributions of the pre-scission neutron multiplicity were analyzed within a stochastic approach based on one-, two- and three-dimensional Langevin equations for the compound nucleus ^{224}Th formed via a complete fusion. In these calculations, dissipation was generated through the chaos weighted wall and window friction formula. Comparison of the theoretical results with the experimental data showed that three-dimensional Langevin equations with dissipation generated through the chaos weighted wall and window friction formula make it possible to reproduce satisfactorily the above-mentioned experimental data.

Key words: fission, evaporation residue cross section, pre-scission neutron multiplicity

PACS: 24.75.+i, 25.70.Jj **DOI:** 10.1088/1674-1137/39/5/054102

1 Introduction

More than half a century after the discovery of fission, the study of fission is still of general interest. The dynamics of fission can be simulated in terms of the multidimensional Langevin equations or multidimensional Fokker-Planck equation (see, for example Refs. [1–14]). The multidimensional Langevin equations and multidimensional Fokker-Planck equation have been extensively and rather successfully used to solve many problems of collective nuclear dynamics in such reactions as fusion fission, induced fission, heavy ion collisions, and quasi-fission (see [10–13] and references therein). The multidimensional Fokker-Planck equation can be solved only using approximate methods, while numerical solution of the multidimensional Langevin equations is possible without almost any approximations. The Langevin dynamics was first used simultaneously by Abe et al. [12] and then by Fröbrich and Gontchar (see their 1998 review [13] and references therein). More recently a review article has been proposed by Zagrebaev and Greiner [14].

One of the most important inputs to the Langevin dynamical calculations is the dissipative property of the nucleus. At present there are several models for dissipation but they give dependencies which are very different from each other. For example, the model of two body dissipation [15] predicts a decrease of dissipation with temperature as T^{-2}, whereas the linear response theory [16, 17] predicts that dissipation increases with temperature, but does not change much with the collective variable. On the other hand, there are certain indications that the nuclear dissipation is deformation dependent. In paper [18], the authors considered deformation dependence for the nuclear dissipation and analyzed the experimental data on the pre-fission multiplicity of neutrons, light charged particles and γ quanta in heavy-ion induced reactions. In the above-mentioned paper [18], the nuclear dissipation coefficient was assumed to be constant up to the saddle point, and that it would sharply increase between saddle and scission points; also many authors considering analysis of the different aspects of nuclear fission assumed a constant nuclear dissipation [19–21].

In this paper, we use the chaos weighted wall and window friction formula in one-, two- and three-dimensional Langevin equations to simulate the dynamics of nuclear fission of the excited compound nucleus ^{224}Th formed in the heavy-ion induced reaction ^{16}O+^{208}Pb. We also reproduce experimental data on the anisotropy of the fission fragment angular distribution, the pre-scission neutron multiplicity, the pre-saddle and post-saddle contributions of the pre-scission neutron multiplicity and the evaporation residue cross section for the compound nucleus ^{224}Th.

The present paper has been arranged as follows. In Section 2, we describe the model and basic equations. The results of calculations are presented in Section 3. Finally, the concluding remarks are given in Section 4.

2 Details of the model

The three-dimensional Langevin model which was

Received 10 September 2014

1) E-mail: m_eslamizadeh@yahoo.com

©2015 Chinese Physical Society and the Institute of High Energy Physics of the Chinese Academy of Sciences and the Institute of Modern Physics of the Chinese Academy of Sciences and IOP Publishing Ltd

developed in Refs. [3–5] is used to simulate the dynamics of the fission of ^{224}Th nucleus formed in heavy ion-induced fusion reaction ^{16}O+^{208}Pb. The nuclear shapes can be described in terms of well-known $\{c,h,\alpha\}$ parameterization [22]. In the present investigation, we use a different asymmetry parameter [4] scaled with elongation $\alpha'=\alpha c^3$. The parameter c describes the elongation of a nucleus. The parameter h determines the change in the neck thickness at a given elongation, while the coordinate α specifies the mass ratio for would-be fragments. In cylindrical coordinates the surface of the nucleus is given by:

$$\rho_{\rm s}^2(z)=\begin{cases} c^{-2}(c^2-z^2)\left(A_{\rm s}c^2+Bz^2+\dfrac{\alpha' z}{c^2}\right), & B\geqslant 0 \\ c^{-2}(c^2-z^2)\left(A_{\rm s}c^2+\dfrac{\alpha' z}{c^2}\right)\exp(Bcz^2), & B<0, \end{cases} \tag{1}$$

where z is the coordinate along the symmetry axis and $\rho_{\rm s}$ is the radial coordinate of the nuclear surface. In Eq. (1) the quantities B and $A_{\rm s}$ are defined by:

$$B=2h+\frac{c-1}{2}, \tag{2}$$

$$A_{\rm s}=\begin{cases} c^{-3}-\dfrac{B}{5}, B\geqslant 0 \\ -\dfrac{4}{3}\dfrac{B}{\exp(Bc^3)+\left(1+\dfrac{1}{2Bc^3}\right)\sqrt{-\pi Bc^3}\,{\rm erf}(\sqrt{-Bc^3})}, & B<0 \end{cases} \tag{3}$$

where erf(x) is the error function.

The evolution of a nucleus undergoing fission is considered within the stochastic approach. The evolution of the collective coordinates can be treated by analogy with the motion of a Brownian particle placed in a viscous heat bath [23, 24]. The heat bath in this picture represents the rest of all the other nuclear degrees of freedom which are assumed to be in thermal equilibrium. In our calculations, we use the set of coupled Langevin equations

$$\begin{aligned} \dot{q}_i &= \mu_{ij}p_j, \\ \dot{p}_i &= -\frac{1}{2}p_jp_k\frac{\partial\mu_{jk}}{\partial q_i}-\frac{\partial F}{\partial q_i}-\gamma_{ij}\mu_{jk}p_k+\theta_{ij}\xi_j, \end{aligned} \tag{4}$$

where $\boldsymbol{q}=(c,h,\alpha')$ are the collective coordinates, $\boldsymbol{p}=(p_c,p_h,p_{\alpha'})$ are their momenta conjugates, $m_{ij}(\|\mu_{ij}\|=\|m_{ij}\|^{-1})$ is the tensor of inertia, $F(\boldsymbol{q})=V(\boldsymbol{q})-a(\boldsymbol{q})T^2$ is the Helmholtz free energy, $V(\boldsymbol{q})$ is the potential energy, γ_{ij} is the friction tensor, $\theta_{ij}\xi_j$ is a random force, θ_{ij} is its amplitude and ξ_j is a random variable that possesses the following statistical properties

$$\langle\xi_i\rangle=0,\ \ \langle\xi_i(t_1)\xi_j(t_2)\rangle=2\delta_{ij}\delta(t_1-t_2). \tag{5}$$

The random force amplitudes are related to the diffusion tensor D_{ij} by the equation $D_{ij}=\theta_{ik}\theta_{kj}$. The diffusion tensor in turn satisfies the Einstein relation $D_{ij}=T\gamma_{ij}$. The heat bath temperature T used in the calculations is determined within the Fermi-gas model as $T=\sqrt{E_{\rm int}/a(\boldsymbol{q})}$, where $E_{\rm int}$ is the intrinsic excitation energy of the nucleus and $a(\boldsymbol{q})$ is the level-density parameter. The deformation dependence of the level density parameter is frequently represented in the form of the expansion [25]

$$a(\boldsymbol{q})=a_{\rm v}A+a_{\rm s}A^{2/3}B_{\rm s}(\boldsymbol{q}), \tag{6}$$

where A is the mass of the fissile nucleus, and $B_{\rm s}$ is the dimensionless functional of the surface-energy in the liquid-drop model. In the present study, we employ the coefficients $a_{\rm v}=0.073$ MeV^{-1} and $a_{\rm s}=0.095$ MeV^{-1}, proposed by Ignatyuk and his co-authors in Ref. [25]. During a random walk along the Langevin trajectory, conservation of energy is satisfied by

$$E^*=E_{\rm int}(t)+E_{\rm coll}(\boldsymbol{q},\boldsymbol{p})+V(\boldsymbol{q})+E_{\rm evap}(t), \tag{7}$$

where E^* is the total excitation energy of the nucleus, $E_{\rm coll}$ is the kinetic energy of the collective motion of the nucleus, which is determined by the formula $E_{\rm coll}=1/2\mu_{ij}(\boldsymbol{q})p_ip_j$, $V(\boldsymbol{q})$ is the potential energy of the compound nucleus, and $E_{\rm evap}(t)$ is the energy carried away by evaporated particles by time t. The potential energy is calculated on the basis of the liquid drop model with allowance for the finite range of nuclear forces [26, 27]. The inertia tensor is calculated in the Werner-Wheeler approximation for the incompressible and irrotational flow [28].

For small elongation before neck formation, we use the chaos weighted wall formula to calculate the friction tensor and after neck formation, we use the chaos weighted wall and window friction formula [29].

$$\gamma_{ij}=\begin{cases} \mu(\boldsymbol{q})\gamma_{ij}^{\rm wall}, \\ \text{for nuclear shapes featuring no neck} \\ \mu(\boldsymbol{q})\gamma_{ij}^{\rm wall}+\gamma_{ij}^{\rm win}, \\ \text{for nuclear shapes featuring a neck} \end{cases} \tag{8}$$

The chaoticity μ is a measure of chaos in the single particle motion and depends on the shape of the nucleus. In the classical picture this can be given as the average fraction of the nucleon trajectories which are chaotic and is evaluated by sampling over a large number of classical trajectories for a given shape of the nucleus. Each such trajectory is identified either as a regular or a chaotic one

by considering the magnitude of its Lyapunov exponent and the nature of its variation with time [30]. The magnitude of chaoticity μ changes from 0 to 1 as the nucleus evolves from a spherical to a deformed shape. $\gamma_{ij}^{\rm wall}$ and $\gamma_{ij}^{\rm win}$ can be written as in [29, 31]. For nuclear shapes featuring no neck

$$\gamma_{ij}^{\rm wall} = \frac{\pi\rho_{\rm m}}{2}\bar{v}\int_{z_{\rm min}}^{z_{\rm max}}\left(\frac{\partial\rho_{\rm s}^2}{\partial q_i}\right)\left(\frac{\partial\rho_{\rm s}^2}{\partial q_j}\right) \times\left[\rho_{\rm s}^2+\left(\frac{1}{2}\frac{\partial\rho_{\rm s}^2}{\partial z}\right)^2\right]^{-1/2}{\rm d}z, \quad (9)$$

and for nuclear shapes featuring a neck

$$\gamma_{ij}^{\rm wall} = \frac{\pi\rho_{\rm m}}{2}\bar{v}\left\{\int_{z_{\rm min}}^{z_{\rm N}}\left(\frac{\partial\rho_{\rm s}^2}{\partial q_i}+\frac{\partial\rho_{\rm s}^2}{\partial z}\frac{\partial D_1}{\partial q_i}\right) \times\left(\frac{\partial\rho_{\rm s}^2}{\partial q_j}+\frac{\partial\rho_{\rm s}^2}{\partial z}\frac{\partial D_1}{\partial q_j}\right)\left[\rho_{\rm s}^2+\left(\frac{1}{2}\frac{\partial\rho_{\rm s}^2}{\partial z}\right)^2\right]^{-1/2}{\rm d}z +\int_{z_{\rm N}}^{z_{\rm max}}\left(\frac{\partial\rho_{\rm s}^2}{\partial q_i}+\frac{\partial\rho_{\rm s}^2}{\partial z}\frac{\partial D_2}{\partial q_i}\right)\left(\frac{\partial\rho_{\rm s}^2}{\partial q_j}+\frac{\partial\rho_{\rm s}^2}{\partial z}\frac{\partial D_2}{\partial q_j}\right) \times\left[\rho_{\rm s}^2+\left(\frac{1}{2}\frac{\partial\rho_{\rm s}^2}{\partial z}\right)^2\right]^{-1/2}{\rm d}z\right\}, \quad (10)$$

$$\gamma_{ij}^{\rm win} = \frac{1}{2}\rho_{\rm m}\bar{v}\left\{\left(\frac{\partial R}{\partial q_i}\frac{\partial R}{\partial q_j}\right)\Delta\sigma+\frac{32}{9}\frac{1}{\Delta\sigma}\frac{\partial V_1}{\partial q_i}\frac{\partial V_1}{\partial q_j}\right\}, \quad (11)$$

where $\rho_{\rm m}$ is the mass density of the nucleus, $\bar{v}$ is the average nucleon speed inside the nucleus, $z_{\rm min}$ and $z_{\rm max}$ are the left and right ends of the nuclear shape, $z_{\rm N}$ is the position of the neck plane that divides the nucleus into two parts, D_1, D_2 are positions of mass centers of the two parts of the fissioning system relative to the center of mass of the whole system, R is the distance between centers of mass of future fragments, $\Delta\sigma$ is an area of the window between two parts of the system and V_1 is the volume of one of the would-be fragments. It should be mentioned that the second term in Eq. (11) takes into account the nucleon flux through the neck connecting the two parts of the fissile nucleus.

Figure 1 shows the components of the friction-tensor as the function of elongation parameter c from the ground state of the fissioning system to its scission along the mean dynamical trajectory. It can be seen that components of the fraction tensor have a smooth behavior.

It should be mentioned that in our dynamical calculations the mean dynamical trajectory is obtained by averaging over a trajectory ensemble. In this case the Langevin equations coincide with the generalized Hamilton equations, since the term responsible for fluctuations, the random force, drops out after averaging. The initial conditions were chosen at the saddle point with $\alpha'=0$ and $p_{\alpha'}=0$ similar to the ground state. Therefore, while the compound nuclei ^{224}Th evolve from the saddle point to the scission point, the average values of the mass asymmetry parameter and the conjugate momentum are identically equal to zero. Consequently, the mean dynamical trajectories lie in the $\alpha'=0$ plane or (c,h) plane. The components $\gamma_{c\alpha'}$ and $\gamma_{h\alpha'}$ are equal to zero in the case $\alpha'=0$.

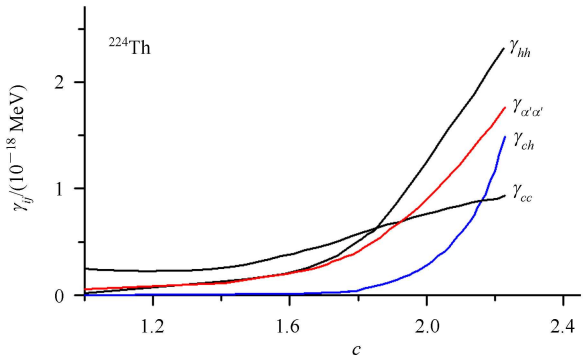

Fig. 1. The nuclear deformation dependence of the friction tensor components along the mean dynamical trajectory for the compound nucleus ^{224}Th as functions of the elongation parameter c.

The Langevin trajectories are simulated starting from the ground state with the excitation energy E^* of the compound nucleus. In the course of evolution of a compound nucleus from the ground state to the scission point along a Langevin trajectory, we take into account the evaporation of light pre-scission particles n, p, α, γ by means of a Monte Carlo procedure. The decay widths for emission n, p, α, γ are calculated at each Langevin time step Δt as in Refs. [32, 33]. The emission of a particle is allowed by asking at each time step along the trajectory whether the ratio of the Langevin time step Δt to the particle decay time $\tau_{\rm part}$ is larger than a random number $\xi(\Delta t/\tau_{\rm part})\xi(0\leqslant\xi\leqslant1))$, where $\tau_{\rm part}=\hbar/\Gamma_{\rm tot}$ and $\Gamma_{\rm tot}=\sum_{\rm v}\Gamma_{\rm v}$. The probabilities of decay via different channels can be calculated by using a standard Monte Carlo cascade procedure where the kind of decay is selected with the weights $\Gamma_{\rm v}/\Gamma_{\rm tot}$ with (v=n, p, α, γ). After emission of a particle of kind v the kinetic energy $\varepsilon_{\rm v}$ of the emitted particle is calculated by hit and miss Monte Carlo procedure. Then the intrinsic excitation energy of the residual mass and spin of the compound nucleus are recalculated and the dynamics are continued. The loss of angular momentum is taken into account by assuming that each neutron, proton, or γ quantum carries away $1\hbar$ while the α particle carries away $2\hbar$.

If the Langevin trajectory has not fissioned and has not been counted as an evaporation residue event after a delay time, when stationary flux over the saddle point is reached, we stop the dynamical calculation and switch

over to the statistical description with a Kramers type fission decay [34].

We obtain average values of the pre-scission particle multiplicity by using the following relation:

$$\langle O\rangle=\frac{\sum\limits_{I=0}^{I=I_{\rm cr}}\sum\limits_{\alpha'=0}^{\alpha'=\alpha'_{\rm f}}\langle O\rangle_{I,\alpha'}(2I+1)P_I}{\sum\limits_{I,\alpha'}(2I+1)P_I}, \tag{12}$$

where $I_{\rm cr}$ and $\alpha'_{\rm f}$ are the critical spin and maximum asymmetry parameter for fusion, respectively. The quantity P_I is the probability of a particle crossing the fission barrier. This is obtained as the ratio of the number of the trajectories crossing the barrier for given α', I and the total number of trajectories chosen.

In the present paper, we use the standard transition state model [35–37] to analyze the fission fragment angular distributions. This model assumes that there is a certain transition configuration for a fissile system that we can use to determine the angular distribution of the fission fragments. There are two assumptions on the position of the transition state and consequently we can consider two variants of the transition state model. These models are the saddle point transition model (SPTS) [35–37] and the scission point transition model (SCTS) [38–40]. Important assumptions of the saddle point transition model are: 1) the mean time of stay of a nucleus in the saddle point region is sufficiently larger than a characteristic time of equilibration of the K mode; 2) the mean time of descent of a nucleus from the saddle to scission is short in comparison with the characteristic time of the equilibration of the K mode; 3) a Gaussian distribution can be considered for K, the projection of I onto the symmetry axis of the nucleus, in the saddle point. In analyzing the fission fragment angular distributions, it is usually assumed that fission fragments travel in the direction of the symmetry axis of the nucleus. Consequently, the fission fragment angular distributions can be determined by three quantum numbers: I, M, K, where I is the spin of a compound nucleus, M is the projection of I on the axis of the projectile ion beam, and K is the projection of I on the symmetry axis of the nucleus. In the case of fusion of spinless ions, we have $M=0$. At fixed values of I and K, the angular distribution can be determined as follows:

$$W(\theta,I,K)=(I+1/2)\left|d^I_{M=0,K}(\theta)\right|^2, \tag{13}$$

where $d^I_{M,K}(\theta)$ is the Wigner rotation function defined in [35], and θ is the angle between the nuclear symmetry axis and the beam axis. At high values of I,$W(\theta,I,K)$ can be approximated as

$$W(\theta,I,K)\approx\frac{I+1/2}{\pi}\times\left[(I+1/2)^2\sin^2\theta-K^2\right]^{1/2}, \tag{14}$$

The experimental observed angular distribution of fission fragments can be calculated by averaging expression Eq. (13) with the distributions of I and K as follows:

$$W(\theta)=\sum_{I=0}^{\infty}\sigma_I\sum_{K=-I}^{I}P(K)W(\theta,I,K), \tag{15}$$

where σ_I and $P(K)$ are the distributions of compound nuclei with respect to the spin and its projection, respectively. In order to calculate the angular distributions of compound nuclei, it is necessary to specify the type of the distributions σ_I and $P(K)$ of the compound nuclei over I and K, respectively. In the saddle point transition state model, an equilibrium distribution of K values is assumed which is determined by the Boltzmann factor $\exp(-E_{\rm rot}/T)$ [37] at the saddle point. Therefore, the equilibrium distribution with respect to K has the form

$$P_{\rm eq}(K)=\frac{\exp(-K^2/(2K_0^2))}{\sum\limits_{K=-I}^{I}\exp(-K^2/(2K_0^2))}, \tag{16}$$

The variance of the equilibrium K distribution K_0 is

$$K_0^2=\frac{T}{\hbar^2}J_{\rm eff},\quad J_{\rm eff}=\frac{J_\parallel J_\perp}{J_\perp-J_\parallel}, \tag{17}$$

where T, $J_\parallel$, and $J_\perp$ are the nuclear temperature and the parallel and perpendicular moments of inertia which were calculated at the saddle point. We can obtain an expression for the angular distribution for a fixed I at preset K_0 by averaging Eqs. (13) and (14) with respect to $P_{\rm eq}(K)$ as follows:

$$\begin{aligned}W(\theta,I)\;&=\;(I+1/2)\frac{\sum\limits_{K=-I}^{I}\left|d^I_{0,K}(\theta)\right|\exp(-K^2/2K_0^2)}{\sum\limits_{K=-I}^{I}\exp(-K^2/2K_0^2)}\\&\approx\sqrt{\frac{2p}{\pi}}\frac{\exp(-p\,\sin^2\theta)J_0(-p\,\sin^2\theta)}{\mathrm{erf}(\sqrt{2p})},\end{aligned} \tag{18}$$

where J_0 is a Bessel function of zero order and $p=(I+1/2)^2/(4K_0^2)$. The anisotropy of the fission fragment angular distribution is given by

$$A=\frac{\langle W(0^0)\rangle}{\langle W(90^0)\rangle}. \tag{19}$$

In the case $P\gg1$ the anisotropy of the fission fragment angular distribution is given by the approximate relation

$$\frac{\langle W(0^0)\rangle}{\langle W(90^0)\rangle}\approx1+\frac{\langle I^2\rangle}{4K_0^2}. \tag{20}$$

It should be stressed that an expression similar to Eq. (18) can be used in a scission point transition model, but factors determined by Eq. (17) should be calculated

at the scission point, and it is assumed that the characteristic time of equilibration of the K mode is much shorter than the descent time from the saddle to the scission point. In this case the equilibration of the K degree of freedom is supposed to be at the scission point.

There are three factors that determine the angular distribution: the effective inertia moments, the nuclear temperatures at the transition states and the initial spin distribution of the compound nuclei.

Assuming complete fusion of the projectile with the target, the spin distribution of the compound nucleus can be described by the formula

$$\frac{\mathrm{d}\sigma(I)}{\mathrm{d}I}=\frac{2\pi}{k^2}\frac{2I+1}{1+\exp\left(\frac{I-I_\mathrm{c}}{\delta I}\right)}, \tag{21}$$

where I_c is the critical spin and δI is the diffuseness. The parameters I_c and δI can be approximated by the following relations [13]:

$$\delta I=\begin{cases}(A_\mathrm{P}A_\mathrm{T})^{3/2}\times10^{-5}[1.5+0.02(E_\mathrm{c.m.}-V_\mathrm{c}-10)]\\ \text{for } E_\mathrm{c.m.}>V_c+10\\ (A_\mathrm{P}A_\mathrm{T})^{3/2}\times10^{-5}[1.5-0.04(E_\mathrm{c.m.}-V_\mathrm{c}-10)]\\ \text{for } E_\mathrm{c.m.}<V_c+10,\end{cases} \tag{22}$$

and

$$I_\mathrm{c}=\sqrt{A_\mathrm{P}A_\mathrm{T}/A_\mathrm{CN}}(A_\mathrm{P}^{1/3}+A_\mathrm{T}^{1/3}) \times(0.33+0.205\sqrt{E_\mathrm{c.m.}-V_\mathrm{c}}), \tag{23}$$

when $0<E_\mathrm{c.m.}-V_\mathrm{c}<120$ MeV; and when $E_\mathrm{c.m.}-V_\mathrm{c}>120$ MeV the term in the last bracket is put equal to 2.5. In Eqs. (22) and (23), V_c is the Coulomb barrier and A_T, A_P and A_CN represent the mass of the target, projectile, and the compound nucleus, respectively. The initial spin of the compound nucleus can be obtained by sampling the above spin distribution function. Fig. 2 shows the calculation results for the partial cross sections as a function of spin for ^{16}O+^{208}Pb. It can be seen from Fig. 2 that at higher center-of-mass energy of the projectile the compound nucleus is formed with a larger value of spin.

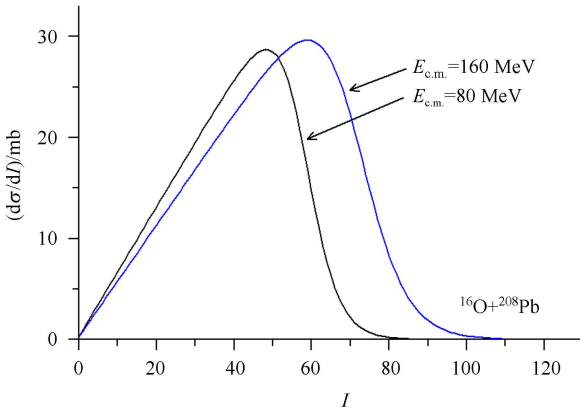

Fig. 2. The partial cross sections as a function of spin for ^{224}Th.

3 Results and discussion

In this paper, we use a stochastic approach based on Langevin equations to calculate the anisotropy of the fission fragment angular distribution, the pre-scission neutron multiplicity, the pre-saddle and post-saddle contributions of the pre-scission neutron multiplicity and the evaporation residue cross section for the compound nucleus ^{224}Th formed in the fusion reaction ^{16}O+^{208}Pb. We use both one-, two- and three-dimensional Langevin equations in our calculations to calculate the above-mentioned experimental data. To calculate the anisotropy of the fission fragment angular distribution, we use the saddle point transition model [35–37] and the scission point transition model [38–40]. In one-dimensional Langevin calculations, we use only the elongation parameter c and the collective coordinates h and α' are set to zero, and in two-dimensional Langevin calculations, we use the elongation parameter c and the collective coordinate h, and α' is set to zero. It should be noted that in order to calculate the anisotropy of the fission fragment angular distribution, an accurate prediction of particle multiplicity is necessary. Therefore, in the present investigation, we considered the deformation effects [41] for calculating the particle emission in our calculations. If we do not consider the deformation effects, we cannot accurately reproduce the experimental data on the anisotropy of the fission fragment angular distribution for ^{224}Th. It should be mentioned that authors in Ref. [41] provided a comprehensive discussion

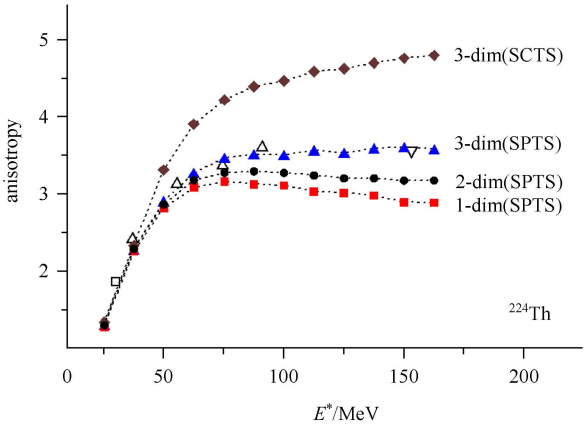

Fig. 3. The anisotropy of fission fragment angular distribution for ^{224}Th calculated with the one-two-, and three-dimensional Langevin equations in the framework SPTS and SCTS model, respectively. The calculated values are connected by dotted lines to guide the eye. The experimental data (open symbols) are from Refs. [42–45].

about the deformation effects on the pre-scission particles multiplicity. Fig. 3 shows the results of the anisotropy of the fission fragment angular distribution along with the experimental data for ^{224}Th.

It is clear from Fig. 3 that the predictions of the scission point transition model for the anisotropy of the fission fragment angular distribution, calculated with the three-dimensional Langevin equations for ^{224}Th, lie higher than the experimental data and the values obtained according to the saddle point transition model.

In order to obtain further insight about the fission dynamics of ^{224}Th, we show in Fig. 4 the mass distributions at saddle and scission points calculated with the three-dimensional Langevin equations in the framework of the SPTS and SCTS models.

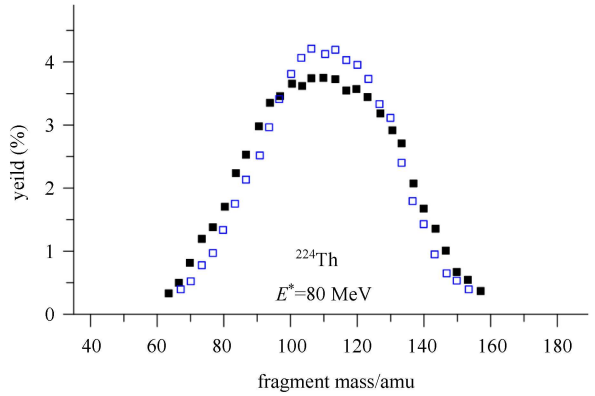

Fig. 4. Mass distribution of fission fragments of ^{224}Th obtained from the three-dimensional Langevin equations at saddle point (filled squares) and scission point (open squares).

It should be stressed that in the reproduction of the experimental data on the anisotropy of the fission fragment angular distribution for ^{224}Th, we consider the particle emission. It should be mentioned that Froebich and Rossner [46] were the first people to use the Langevin-type model to study the influence of pre-saddle particles on the anisotropy of the fission fragment angular distribution, and pointed out its importance for interpreting the anisotropy data, in particular at high energy.

Figure 5 shows the results of the anisotropy of the fission fragment angular distributions calculated in the framework SPTS model for ^{224}Th with the one-, two- and three-dimensional Langevin equations without considering the particle emission. It is clear from Fig. 5 that the results of the three-dimensional Langevin equations for the anisotropy of the fission fragment angular distribution lie somewhat below the experimental data.

It can be seen from Figs. 3 and 5 that the values of the anisotropy of the fission fragment angular distribution calculated in the framework SPTS model with the one-, two and three-dimensional Langevin equations are very close at smaller excitation energies, though at higher excitations energies, the predictions of three-dimensional Langevin equations are higher than those obtained with the one-, and two-dimensional Langevin equations and consequently are in better agreement with the experimental data. The difference between predictions of the one-, two- and three-dimensional Langevin equations can be explained as follows: in the one-dimensional case there is only one transition state for each spin, in contrast to the two- and three-dimensional case where the ensemble of transition points exist, and also the mean nuclear temperature at the saddle or scission points are different from each other in the one-, two- and three-dimensional Langevin calculations. It should be mentioned that the nuclear temperature at the saddle point or at the scission point is tightly bound with the mean pre-saddle or pre-scission neutron multiplicity and consequently with the nuclear dissipation. The results of pre-scission neutron multiplicity, the pre-saddle and post-saddle (saddle to scission) contributions (ν_{gs} and ν_{ss} respectively) of the pre-scission neutron multiplicity calculated for ^{224}Th with the one- and three-dimensional Langevin equations are shown in Fig. 6. It can be seen from Fig. 6 that the pre-scission neutron multiplicity values calculated with the one- and three-dimensional Langevin equations are close at smaller excitation energies, though at higher excitation energies the predictions of three-dimensional Langevin equations are lower than those obtained with the one-dimensional Langevin equations and consequently are in better agreement with the experimental data.

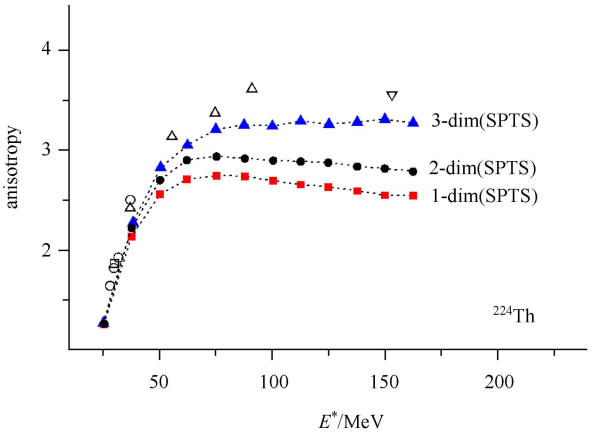

Fig. 5. Same as Fig. 3, but without considering the particle emission.

It is also clear from Fig. 6 that the post-saddle contribution at low excitation energies is very small, but increases at higher excitation energies. In order to obtain further insight into the dynamics of fission, we also calculate the percentage yield of the pre-scission neutron multiplicities as a function of the elongation parameter

c for the compound nucleus ^{224}Th at excitation energy equal to 80 MeV.

Figure 7 shows the results of the percentage yield of the pre-scission neutron multiplicities for ^{224}Th calculated with the three-dimensional Langevin equations. It is clear from Fig. 7 that an appreciable part of the pre-scission neutron is evaporated from the nearly spherical compound nucleus at an early stage of fission process before the saddle point is reached.

Apart from the above-mentioned arguments, it can be mentioned that in the one-dimensional case, the fissioning system can oscillate only in the fission direction, and the energy is transferred only between the elongation degree of freedom and the heat bath. But in the three-dimensional calculations the energy can be transferred not only between the elongation variable and the heat bath, but also between the elongation variable and the other collective variables. The combination of all these effects leads to the differences between the one-, two- and three-dimensional calculations seen in Figs. 3, 5 and 6.

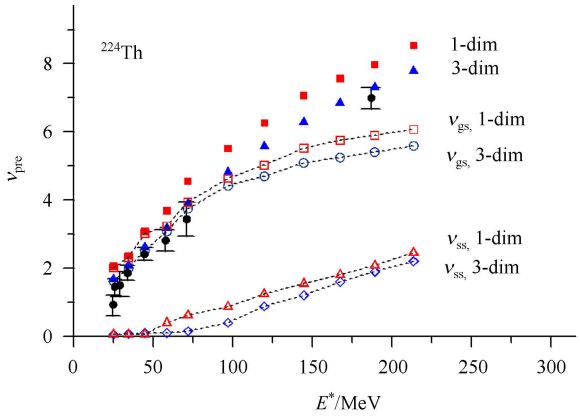

Fig. 6. The calculated pre-scission neutron multiplicity pre-saddle and post-saddle contributions of the pre-scission neutron multiplicity for ^{224}Th at different excitation energies. The experimental data (filled circles) are from refs. [47, 48].

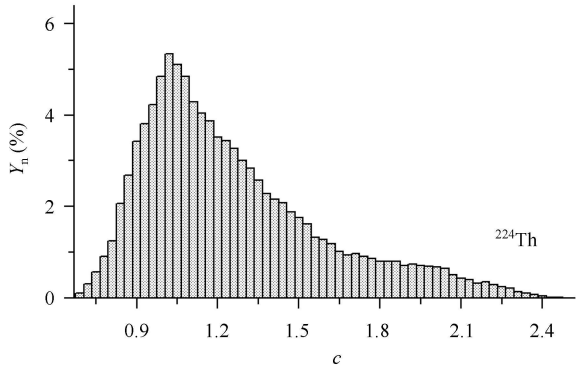

Fig. 7. Percentage yield of the pre-scission neutron multiplicities as a function of the elongation parameter c for ^{224}Th at an excitation energy equal to 80 MeV.

We also calculated the energy dependencies of the evaporation residue cross section, σ_{ER}, for ^{224}Th with the one- and three-dimensional Langevin equations. Fig. 8 shows the energy dependencies of σ_{ER} for ^{224}Th.

It can be seen from Fig. 8 that the evaporation residues cross section values calculated with the one- and three-dimensional Langevin equations are different from each other and the predictions of three-dimensional Langevin equations are lower than those obtained with the one-dimensional Langevin equations. It is also clear from Fig. 8 that the results of the three-dimensional Langevin equations are in better agreement with the experimental data.

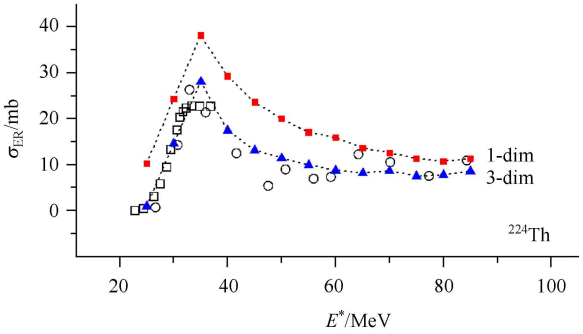

Fig. 8. The evaporation residues cross section calculated with the one- and three-dimensional Langevin equations. The calculated values are connected by dotted lines to guide the eye. The experimental data (open symbols) are from Refs. [42, 49].

4 Conclusions

The anisotropy of the fission fragment angular distribution, the pre-scission neutron multiplicity, the pre-saddle and post-saddle contributions of the pre-scission neutron multiplicity and the evaporation residue cross section have been calculated for the compound nucleus ^{224}Th formed in heavy ion-induced fusion reaction ^{16}O+^{208}Pb based on one-, two- and three-dimensional Langevin equations.

In our calculations, we used the chaos weighted wall and window friction formula in the Langevin equations to reproduce the above mentioned experimental data. Comparison of the theoretical results with the experimental data show that the anisotropy of the fission fragment angular distribution and the mean pre-scission neutron multiplicity calculated with the one- and three-dimensional Langevin equations are very close at smaller excitation energies, though at higher excitation energies the predictions of three-dimensional Langevin equations are in better agreement with the experimental data.

Furthermore, the results of the calculations of the evaporation residue cross section for ^{224}Th indicate that the three-dimensional calculations give lower values than in the one-dimensional case, and consequently are in better agreement with the experimental data. According to the obtained results, it can be concluded that the neck thickness and asymmetry degrees of freedom decrease the pre-scission neutron multiplicity and the evaporation residues cross section, and increase the anisotropy of the fission fragment angular distribution. It should be mentioned that the authors in Ref. [3] have applied the surface-plus-window dissipation with reduction coefficient $0.25 \leqslant k_s \leqslant 0.5$ and analyzed experimental data of the different features of the fission of excited compound nuclei. In other words, the authors in Ref. [3] assumed the reduction coefficient as a free parameter in their calculations, but, in the present investigation, we did not consider any free parameters to reproduce experimental data.

The support of the Research Committee of the Persian Gulf University is greatly acknowledged.

References

1 Nadtochy P N, Ryabov E G, Gegechkori A E, Anischenko Yu A, Adeev G D. Phys. Rev. C, 2014, **89**: 2806
2 Eslamizadeh H. Ann. Nuc. Energy, 2011, **38**: 2806
3 Nadtochy P N, Adeev G D, Karpov A V. Phys. Rev. C, 2002, **65**: 064615
4 Karpov A V, Nadtochy P N, Vanin D V, Adeev G D. Phys. Rev. C, 2001, **63**: 054610
5 Karpov A V, Hiryanov R M, Sagdeev A V, Adeev G D. J. Phys. G: Nucl. Part. Phys., 2007, **34**: 255
6 Eslamizadeh H. J. Phys. G: Nucl. Part. Phys., 2013, **40**: 095102
7 Eslamizadeh H. Chinese Phys. C, 2014, **38**: 064101
8 Eslamizadeh H. Pramana, J. Phys., 2013, **80**: 621
9 Anischenko Ya A, Gegechkori A E, Adeev G D. Acta Phys. Pol. B, 2011, **42**: 493
10 Eslamizadeh H. Chinese Phys. C, 2010, **34**:1714
11 Adeev G D, Pashkevich V V. Nucl. Phys. A, 1989, **502**: 405
12 Abe Y, Ayik S, Reinhard P G, Suraud E. Phys. Rep., 1996, **275**: 49
13 Fröbrich P, Gontchar I I. Phys. Rep., 1998, **292**: 131
14 Zagrebaev V, Greiner W. Clusters in Nuclei - Vol. 1, Lecture Notes in Physics 818, 2010. 267
15 Hilscher D, Rossner H. Ann. Phys., 1992, **17**: 471
16 Yamaji S, Hofmann H, Samhammer R. Nucl. Phys. A, 1988, **475**: 487
17 Yamaji S, Ivanyuk F A, Hofmann H. Nucl. Phys. A, 1997, **612**: 1
18 Fröebrich P, Gontchar I I. In: Proc. Int. School-Seminar on Heavy-Ion Phys. (Dubna, Russia) ed Oganessian Y T et al. (Dubna: JINR), 1993, 344
19 YE W, YANG H W, WU F. Phys. Rev. C, 2008, **77**: 011302
20 YE W. Phys. Rev. C, 2010, **81**: 011603
21 Bourique B, Abe Y, Boilley D. Comp. Phys. Comm., 2004, **159**: 1
22 Brack M, Damgaard J, Jensen A S, Puli H C, Strutinsky V M. Rev. Mod. Phys., 1972, **44**: 320
23 Kramers H A. Physica (Amesterdam), 1940, **7**: 284
24 Abe Y, Gregoire C, Delagrange H. J. Phys. C, 1986, **4**: 329
25 Ignatyuk A V, Itkis M G, Okolovich V N, Smirenkin G N, Tishin A S. Yad. Fiz., 1975, **21**: 1185
26 Krappe H J, Nix J R, Sierk A J. Phys. Rev. C, 1979, **20**: 992
27 Sierk A J. Phys. Rev. C, 1986, **33:** 2039
28 Davies K T R, Sierk A J, Nix J R. Phys. Rev. C, 1976, **13**: 2358
29 Pal S, Mukhopadhyay T. Phys. Rev. C, 1998, **57**: 210
30 Blocki J, Brut F, Srokowski T, Swiatecki W J. Nucl. Phys. A, 1992, **545**: 511
31 Vanin D V, Kosenko G I, Adeev G D. Phys. Rev. C, 1999, **59**: 2114
32 Blann M. Phys. Rev. C, 1980, **21**: 1770
33 Lynn J E. The Theory of Neutron Resonance Reactions. Clarendon: Oxford, 1968, 325
34 Mavlitov N D, Fröbrich P, Gontchar I I. Z. Phys. A, 1992, **342**: 195
35 Vandenbosch R, Huizenga J R. Nuclear Fission. New York: Academic, 1973
36 Bohr A. In: Proc of the United Nations International Conference on the Peaceful Uses of Atomic Energy. United Nations, New York, 1956, **2**: 151
37 Halpern I, Strutinsky V M. In: Proc of the United Nations International Conference on the peaceful Uses of Atomic Energy. United Nations, Geneva, 1958, **15**: 408
38 Rossner H H, Huizenga J R, Schröder W U. Phys. Rev. Lett., 1984, **53**: 38
39 Bond P D. Phys. Rev. C, 1985, **32**: 471
40 Rossner H H, Huizenga J R, Schröder W U. Phys. Rev. C, 1986, **33**: 560
41 WANG N, YE W. Phys. Rev. C, 2013, **87**: 051601
42 Morton C R et al. Phys. Rev. C, 1995, **52**: 243
43 Vulgaris E, Grodzins L, Steadman S G, Ledoux R. Phys. Rev. C, 1986, **33**: 2017
44 Back B B et al. Phys. Rev. C, 1985, **32**: 195
45 Vaz L C et al. Z Phys. A, 1984, **315**: 169
46 Froebrich P and Rossner H. Z. Phys. A, 1994, **349**: 99
47 Rossner H et al. Phys. Rev. C, 1992, **45**: 719
48 Hinde D J et al. Phys. Rev. C, 1992, **45**: 1229
49 Brinkman K T et al. Phys. Rev. C, 1994, **50**: 309